26th IMEKO TC4 International Symposium
24th International Workshop on ADC and DAC Modelling and Testing
IMEKO TC-4 2023
Pordenone, Italy / September 20-21, 2023

Accurate Frequency and Damping Factor Estimation by Means of an Improved Three-point Interpolated DFT Algorithm

Daniel Belega[1], Dario Petri[2], Dominique Dallet[3]

[1]*Department of Measurements and Optical Electronics, University Politehnica Timisoara, Bv. V. Parvan, Nr. 2, 300223, Timisoara, Romania, email: daniel.belega@upt.ro*
[2]*Department of Industrial Engineering, University of Trento, Via Sommarive, 9, 38123, Trento, Italy, email: dario.petri@unitn.it*
[3]*IMS Laboratory, Bordeaux INP, University of Bordeaux, CNRS UMR5218, 351 Cours de la Libération, Bâtiment A31, 33405, Talence Cedex, France, email: dominique.dallet@ims-bordeaux.fr*

***Abstract* – In this paper an algorithm for frequency and damping factor estimation of a real-valued noisy damped sinusoid is proposed. It is an extension of the three-point Interpolated Discrete Fourier Transform (3p-IpDFT) undamped sinusoid frequency estimator based on Maximum Sidelobe Decay (MSD) windows. Analytical expressions for the frequency and the damping factor estimators are provided and the related estimation errors due to the contribution of the spectral image component are derived and compensated. The accuracies of the proposed algorithm and other state-of-the-art frequency-domain based algorithms are compared to each other through computer simulations.**

I. INTRODUCTION

Damped sinusoids have a relevant role in many application areas such as radar, nuclear magnetic resonance, optics, and mechanics [1]-[4]. Quite often the signal parameters need to be estimated accurately and in real-time. To that aim the so-called Interpolated Discrete-Time Fourier Transform (IpDTFT) algorithms are often employed [3]-[9]. These algorithms allow to reduce the picket-fence effect on the estimated signal parameters due to the finite number of samples used in the time-frequency transformation. Specifically, the IpDTFT algorithms estimate the signal frequency and the damping factor by interpolating two or more relevant DTFT samples of the analyzed signal [3]-[9]. Moreover, to reduce the detrimental effect of the spectral interference from other spectral tones, including the image components, the acquired signal is multiplied by a suitable window [10]. The Maximum Sidelobe Decay (MSD) cosine windows [11] are often used since they ensure both high spectral leakage suppression and allow to estimate the unknown parameters using simple analytical expressions [9]. When a few sinusoids cycles are analyzed, more than two interpolation points are used in order to compensate the effect of spectral leakage from the fundamental image component. A three-point Interpolated Discrete Fourier Transform (3p-IpDFT) algorithm based on the rectangular window has been proposed in [12] for undamped sinusoid frequency estimation. Its analytical expression has been derived in [13] and then it has been extended to signals weighted by cosine windows in [14]. In this paper that algorithm is further extended to real-valued noisy damped sinusoids weighted by MSD windows. The expressions for both 3p-IpDFT frequency and damping factor estimators are firstly derived. Then the contribution of the spectral image component to the derived estimators is analyzed and the obtained expressions are used to improve estimation accuracy. The proposed procedure is called the improved 3p-IpDFT (3p-IpDFTi) algorithm, and its accuracy is compared with that of other state-of-the-art frequency domain-based algorithms.

II. THE PROPOSED 3P-IPDTFTI ALGORITHM

The analyzed discrete-time noisy damped sinusoid is modelled as:

$$y(m) = Ae^{-\frac{2\pi}{M}\alpha m}\cos\left(2\pi\frac{\vartheta}{M}m+\phi\right)+e(m)$$
$$= x(m)+e(m),\quad m=0,1,2,\ldots,M-1, \qquad (1)$$

where $x(\cdot)$ is the noise free damped sinusoid of amplitude A, normalized frequency ϑ, phase ϕ, and normalized damping factor α, while $e(\cdot)$ is an additive white Gaussian noise with zero mean and variance σ_n^2. M is the acquisition length.

The normalized damping factor α has been selected as signal parameter for symmetry with the definition of the normalized frequency ν, which also represents the number of analyzed signal cycles and it is expressed as:

$$\vartheta = l+\delta, \qquad (2)$$

where l is the rounded value of ϑ, and δ ($-0.5 \le \delta < 0.5$) is the rounding error, which corresponds to the inter-bin frequency location. $\delta = 0$ if coherent sampling occurs.

To reduce the spectral leakage contribution on the frequency and the damping factor estimates, the acquired signal is multiplied by the H-term MSD window and the analyzed signal becomes $y_w(m) = y(m) \cdot w(m)$.

The DTFT of the noise free weighted damped sinusoid $x_w(m)$ is given by:

$$X_w(\lambda) = \tilde{X}_w(\lambda) + \tilde{X}_{iw}(\lambda), \tag{3}$$

where $\tilde{X}_w(\lambda)$ and $\tilde{X}_{iw}(\lambda)$ are the transforms of the fundamental component and the spectral image of the weighted damped sinusoid $x_w(m) = x(m) \cdot w(m)$, respectively. The related expressions are [9]:

$$\tilde{X}_w(\lambda) \cong \frac{(2H-2)!}{2^{2H}} \frac{AM}{\pi} \frac{\left(1-e^{-2\pi(\alpha+j(\lambda-\vartheta))}\right)e^{j\phi}}{(\alpha+j(\lambda-\vartheta))\prod_{h=1}^{H-1}\left[(\alpha+j(\lambda-\vartheta))^2+h^2\right]}, \tag{4a}$$

and

$$\tilde{X}_{iw}(\lambda) \cong \frac{(2H-2)!}{2^{2H}} \frac{AM}{\pi} \frac{\left(1-e^{-2\pi(\alpha+j(\lambda+\vartheta))}\right)e^{-j\phi}}{(\alpha+j(\lambda+\vartheta))\prod_{h=1}^{H-1}\left[(\alpha+j(\lambda+\vartheta))^2+h^2\right]}. \tag{4b}$$

The 3p-IpDFT algorithm exploits the following interpolation function [14]:

$$h = H \frac{Y_w(l+1)-Y_w(l-1)}{Y_w(l-1)-2Y_w(l)+Y_w(l+1)}. \tag{5}$$

Since both the spectral image component and wideband noise often provides minor contributions (5) can be written as:

$$h \cong H \frac{\tilde{X}_w(l+1)-\tilde{X}_w(l-1)}{\tilde{X}_w(l-1)-2\tilde{X}_w(l)+\tilde{X}_w(l+1)}. \tag{6}$$

By using (4a), after some algebra the following relationships are derived:

$$\begin{aligned} \tilde{X}_w(l-1) &\cong \frac{\alpha-j\delta+j(H-1)}{\alpha-j\delta-jH}\tilde{X}_w(l), \\ \tilde{X}_w(l+1) &\cong \frac{\alpha-j\delta-j(H-1)}{\alpha-j\delta+jH}\tilde{X}_w(l). \end{aligned} \tag{7}$$

By replacing (7) into (6), after some manipulations we obtain:

$$h \cong \delta + j\alpha. \tag{8}$$

which shows that the 3p-IpDFT inter-bin frequency location and damping factor estimators can be obtained as:

$$\hat{\delta} = Re\{h\} \text{ and } \hat{\alpha} = Im\{h\}, \tag{9}$$

where $Re\{\cdot\}$ and $Im\{\cdot\}$ are the real- and imaginary-part operators.

The following Proposition provides the contribution to (9) of the spectral image component.

Proposition:

The contribution of the spectral image component on the estimators of the inter-bin frequency location δ and the damping factor α returned by the 3p-IpDFT algorithm based on the H-term MSD window is given by:

$$\begin{aligned} \Delta\delta + j\Delta\alpha \cong -2(l+\delta)\frac{\alpha-j\delta}{\alpha+j\delta+j2l} \cdot \frac{1-e^{-2\pi(\alpha+j\delta)}}{1-e^{-2\pi(\alpha-j\delta)}} \\ \times \frac{\prod_{h=1}^{H}[(\alpha-j\delta)^2+h^2]}{\prod_{h=1}^{H}[(\alpha+j\delta+j2l)^2+h^2]} \cdot e^{-j2\phi}, \end{aligned} \tag{10}$$

where $\Delta\delta = \hat{\delta} - \delta$ and $\Delta\alpha = \hat{\alpha} - \alpha$. The proof of this Proposition is given in the Appendix.

Expression (10) allows to infer the following remarks:

- if the signal phase changes while the other parameters are kept constant, as it often occurs in practice due to noncoherent sampling, the estimation errors $\Delta\delta$ and $\Delta\alpha$ exhibit two in quadrature sinewave like behaviors;
- the estimation errors $\Delta\delta$ and $\Delta\alpha$ decreases as ϑ increases.

Fig. 1 shows the inter-bin frequency location (Fig. 1(a)) and the damping factor (Fig. 1(b)) estimation errors returned by simulations and by (10) as a function of the signal phase ϕ, which varies in the range [0, 2π) rad with a step of $\pi/20$ rad. A noise free damped sinusoid with A = 1 p.u., ϑ = 3.3 cycles, α = 1, and M = 512 samples is considered and the rectangular or the two-term MSD (or Hann) window are applied.

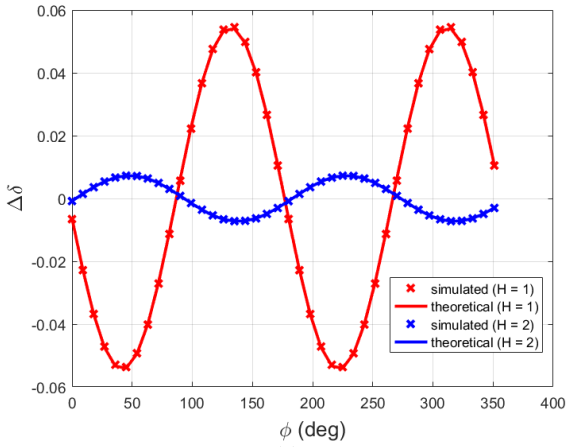

(a)

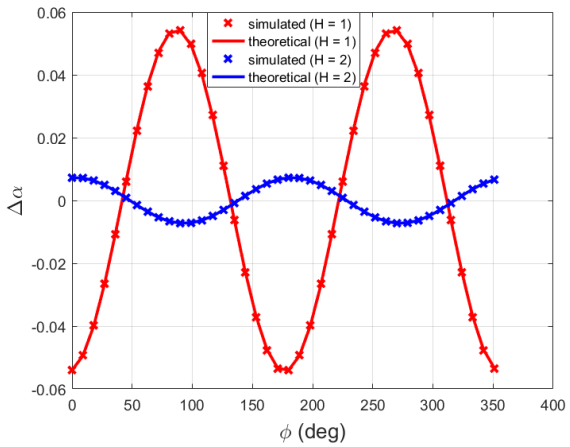

(b)

Fig. 1. Real-valued noise-free damped sinusoid: simulation and theoretical results (10) for the contribution of the spectral image component to the estimated frequency $\Delta\delta$ (a) and damping factor $\Delta\alpha$ (b) versus the signal phase ϕ. Sinusoid parameters A = 1 p.u., ϑ = 3.3 cycles, α = 1, and M = 512 samples. Rectangular (H = 1) or Hann (H = 2) windows.

As we can see, the agreement between the theory and the simulations is very good. For the contribution $\Delta\delta$, the maximum differences between the theoretical and simulated results are $6.3 \cdot 10^{-4}$ and $3.3 \cdot 10^{-5}$ when $H = 1$ and $H = 2$, respectively. Similarly, the contribution $\Delta\alpha$ exhibits maximum differences equal to $5.8 \cdot 10^{-4}$ and $3.0 \cdot 10^{-5}$ when $H = 1$ and $H = 2$, respectively.

Expression (10) enables the improvement of the algorithm accuracy. The derived procedure – called the 3p-IpDFTi algorithm – requires to perform the following steps:

Step 1: acquire M samples of the signal $y(m)$ to be analyzed

Step 2: compute the DFT of the weighted signal $y_w(m)$

Step 3: determine the integer part of the acquired signal cycles l

Step 4: apply the 3p-IpDFT algorithm and compute the estimators $\hat{\delta}$ and $\hat{\alpha}$ using (9)

Step 5: compute $\hat{\phi} = angle\{\gamma\}$, where:

$$\gamma = \frac{(\hat{\alpha}-j\hat{\delta})\prod_{h=1}^{H-1}\left[(\hat{\alpha}-j\hat{\delta})^2+h^2\right]}{1-e^{-2\pi(\hat{\alpha}-j\hat{\delta})}} Y_w(l),$$

Step 6: compute the estimation errors $\Delta\delta$ and $\Delta\alpha$ using (10) applied to the estimated values $\hat{\delta}$, $\hat{\alpha}$, and $\hat{\phi}$

Step7: compute the compensated estimates $\hat{\delta}_c = \hat{\delta} - \Delta\delta$ and $\hat{\alpha}_c = \hat{\alpha} - \Delta\alpha$.

III. ACCURACY ASSESSMENT AND COMPARISON

In this Section the Root Mean Squares (*RMSE*s) of the proposed 3p-IpDFTi algorithm, the classical 2p-IpDFT algorithm [8], the Aboutanios algorithm [4], the 3p-IpDFT algorithm, and the 3p-RVCI-(*H*-1) algorithm [3] are compared to each other. Both the rectangular and the Hann windows are considered for signal weighting.

Undistorted or harmonically distorted noisy damped sinusoids with amplitude $A = 1$ p.u. and normalized damping factor $\alpha = 1$ are analyzed. A white Gaussian noise with zero mean and variance corresponding to $SNR = 40$ dB is added to the signal and 10,000 runs of $M = 512$ samples each with the signal phase ϕ randomly chosen in the range $[0, 2\pi)$ rad are performed for each considered value of the number of analyzed cycles ϑ. The obtained *RMSE*s are reported in Figs. 2 and 3 as a function of ϑ, which varies in the range [1.5, 8] cycles with a step of 0.1 cycles.

Fig. 2 shows the *RMSE*s for the inter-bin frequency location (Fig. 2(a)) and the damping factor (Fig. 2(b)) estimates obtained when a noisy undistorted damped sinusoid is analyzed, and the rectangular window is used. Thanks to the compensation of the contribution from the spectral image component, the proposed 3p-IpDFTi algorithm well outperforms the others.

Fig. 3 shows the *RMSE*s for the inter-bin frequency location (Fig. 3(a)) and the damping factor (Fig. 3(b)) estimates as a function of *SNR* when $\vartheta = 3.3$ cycles and $\alpha = 1$. *SNR* varies in the range [0, 60] dB with a step of 5 dB. When *SNR* is smaller than about 10 dB the 3p-RVCI-0 algorithm is not able to provides accurate *RMSE*s estimates.

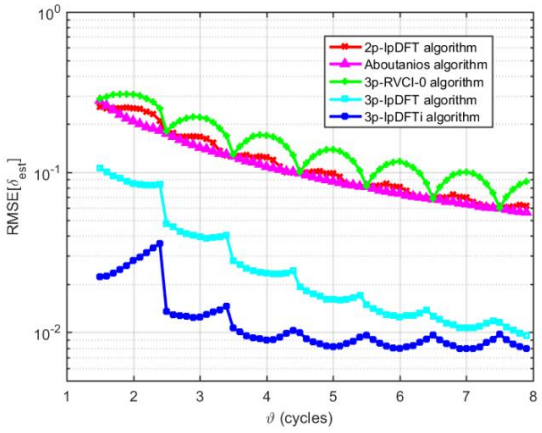

(a)

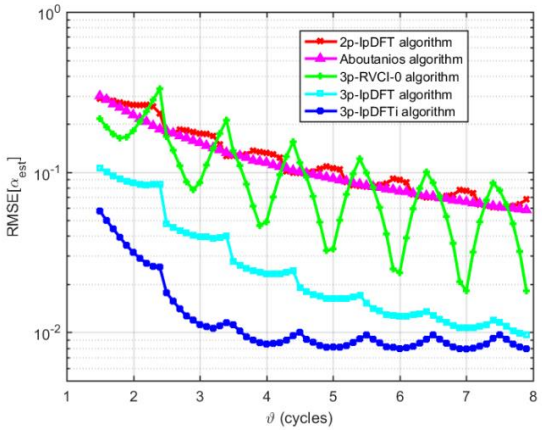

(b)

Fig. 2. Real-valued noisy damped sinusoids: *RMSE*s of the frequency δ (a) and the damping factor α (b) estimates returned by the considered algorithms versus the number of analyzed cycles ϑ. Damping factor $\alpha = 1$, $SNR = 40$ dB, phase at random, and $M = 512$ samples. Rectangular window.

The square root of the Cramér-Rao Lower Bound (CRLB) is also shown in the figure to enable a visual assessment of the algorithm efficiency [15].

In Fig. 3 it can be observed that when *SNR* is greater than about 10 dB the proposed 3p-IpDFTi algorithm outperforms the others since it compensates the contribution of the spectral image component. However, when *SNR* is greater than about 40 dB the residual contribution prevails on the effect of wideband noise. The other considered algorithms exhibit a similar behavior, but at lower *SNR* thresholds. When *SNR* is smaller than about 10 dB outliers due to noise occur [16].

Fig. 4 shows the *RMSE*s for the inter-bin frequency location (Fig. 4(a)) and the damping factor (Fig. 4(b) estimates obtained when a noisy harmonically distorted damped sinusoid is analyzed, and the Hann window is used. The signal is affected by a 2nd and a 3rd damped harmonics with amplitudes equal to 0.1 p.u. and 0.05 p.u., respectively, and damping factors equal to 1.2 and 1.5, respectively.

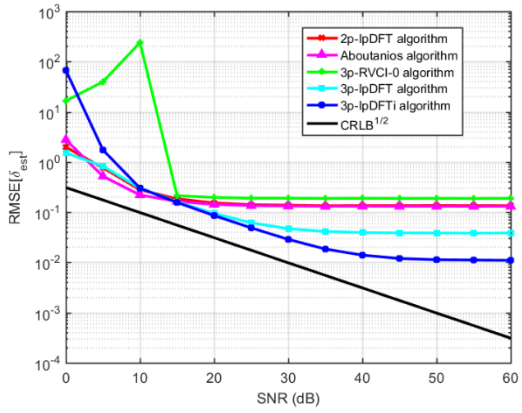

(a)

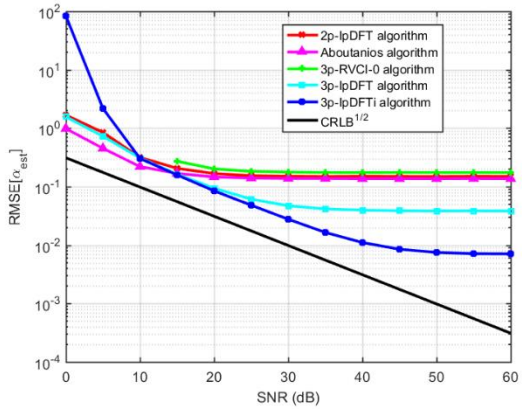

(b)

Fig. 3. Real-valued noisy damped sinusoids: *RMSE*s of the frequency δ (a) and the damping factor α (b) estimates returned by the considered algorithms versus *SNR* when the number of analyzed cycles $\vartheta = 3.3$ cycles, the damping factor $\alpha = 1$, phase at random, and $M = 512$ samples. Rectangular window. The $\sqrt{CRLB}$ is also shown.

As we can see, the proposed 3p-IpDFTi algorithm outperforms the others when less than about 3.5 cycles are analyzed. For greater values of ϑ the 3p-RVCI-1 algorithm provides a slightly better inter-bin frequency location. Conversely, the 2p-IpDFT and the Aboutanios algorithms return a bit more accurate damping factor estimates, while the 3p-RVCI-1 algorithm exhibits poor accuracy.

III. CONCLUSIONS

In this paper the 3p-IpDFTi algorithm based on the MSD windows has been proposed for frequency and damping factor estimation of a real-valued noisy damped sinusoid. The algorithm compensates the contribution of the spectral image component on the returned estimates, so assuring a better accuracy than the classical 2p-IpDFT [8], the Aboutanios [4], and the 3p-RVCI-(*H*-1) [3] algorithms when only few signal cycles are analyzed. Due to its implementation simplicity, the 3p-IpDFTi algorithm is suitable for real-time, fast-response damped sinusoid parameter estimation.

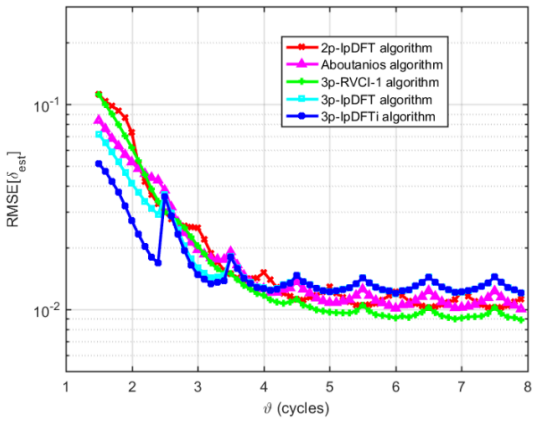

(a)

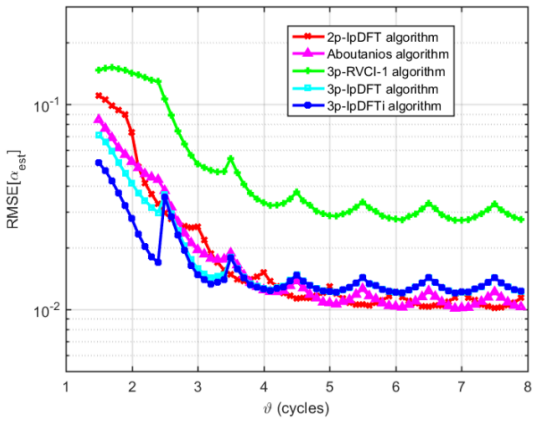

(b)

Fig. 4. Real-valued noisy harmonically distorted damped sinusoids: *RMSE*s of the frequency δ(a) and the damping factor α (b) estimates returned by the considered algorithms versus the number of analyzed cycles ϑ. Damping factor $\alpha = 1$, *SNR* = 40 dB, phase at random, and $M = 512$ samples. 2nd and 3rd harmonics with damping factors equal to 1.2 and 1.5 and amplitudes equal to 10% and 5% of the fundamental. Hann window.

APPENDIX

PROOF OF THE PROPOSITION

For a noise free signal, by using (3), the interpolation function (5) becomes:

$$h = H\frac{\tilde{X}_w(l+1)+\tilde{X}_{iw}(l+1)-\tilde{X}_w(l-1)-\tilde{X}_{iw}(l-1)}{\tilde{X}_w(l-1)+\tilde{X}_{iw}(l-1)-2\tilde{X}_w(l)-2\tilde{X}_{iw}(l)+\tilde{X}_w(l+1)+\tilde{X}_{iw}(l+1)} = H\frac{\tilde{X}_w(l+1)-\tilde{X}_w(l-1)}{\tilde{X}_w(l-1)-2\tilde{X}_w(l)+\tilde{X}_w(l+1)}\frac{1+\frac{\tilde{X}_{iw}(l+1)-\tilde{X}_{iw}(l-1)}{\tilde{X}_w(l+1)-\tilde{X}_w(l-1)}}{1+\frac{\tilde{X}_{iw}(l-1)-2\tilde{X}_{iw}(l)+\tilde{X}_{iw}(l+1)}{\tilde{X}_w(l-1)-2\tilde{X}_w(l)+\tilde{X}_w(l+1)}}. \quad \text{(A.1)}$$

If enough sinusoid cycles are observed, the contribution of the spectral image on the DFT samples is small, and so we have:

$\left|\frac{\tilde{X}_{iw}(l-1)-2\tilde{X}_{iw}(l)+\tilde{X}_{iw}(l+1)}{\tilde{X}_w(l-1)-2\tilde{X}_w(l)+\tilde{X}_w(l+1)}\right| \ll 1$. By using the approximation $(1+x)^{-1} \cong 1-x$, when $|x| << 1$, and neglecting the product of spectral image components, (A.1) becomes:

$$h \cong H\frac{\tilde{X}_w(l+1)-\tilde{X}_w(l-1)}{\tilde{X}_w(l-1)-2\tilde{X}_w(l)+\tilde{X}_w(l+1)}(1+\varepsilon), \qquad (A.2)$$

where:

$$\varepsilon \cong 1+\frac{\tilde{X}_{iw}(l+1)-\tilde{X}_{iw}(l-1)}{\tilde{X}_w(l+1)-\tilde{X}_w(l-1)}-\frac{\tilde{X}_{iw}(l-1)-2\tilde{X}_{iw}(l)+\tilde{X}_{iw}(l+1)}{\tilde{X}_w(l-1)-2\tilde{X}_w(l)+\tilde{X}_w(l+1)}$$

From (A.2) and (8) we obtain:

$$\hat{h} = \hat{\delta} + j\hat{\alpha} = (\delta + j\alpha)(1+\varepsilon). \qquad (A.3)$$

From which it results:

$$\Delta\delta + j\Delta\alpha = (\delta + j\alpha)\varepsilon. \qquad (A.4)$$

From (4a) we achieve:

$$\tilde{X}_{iw}(l-1) \cong \frac{\alpha+j(\delta+2l)+j(H-1)}{\alpha+j(\delta+2l)-jH}\tilde{X}_{iw}(l),$$
$$\tilde{X}_{iw}(l+1) \cong \frac{\alpha+j(\delta+2l)-j(H-1)}{\alpha+j(\delta+2l)+jH}\tilde{X}_{iw}(l). \qquad (A.5)$$

From (7) and (A.5), after some algebra the expression of ε becomes:

$$\varepsilon \cong 2\frac{j(l+\delta)}{\alpha-j\delta}\frac{(\alpha-j\delta+jH)(\alpha-j\delta-jH)}{(\alpha+j(\delta+2l)+jH)(\alpha+j(\delta+2l)-jH)}\frac{\tilde{X}_{iw}(l)}{\tilde{X}_w(l)}. \qquad (A.6)$$

From (4a) and (4b) it follows:

$$\frac{\tilde{X}_{iw}(l)}{\tilde{X}_w(l)} = \frac{1-e^{-2\pi(\alpha+j\delta)}}{1-e^{-2\pi(\alpha-j\delta)}}\frac{\alpha-j\delta}{\alpha+j(\delta+2l)}\frac{\prod_{h=1}^{H}[(\alpha-j\delta)^2+h^2]}{\prod_{h=1}^{H}[(\alpha+j\delta+j2l)^2+h^2]}e^{-j2\phi} \qquad (A.7)$$

Finally, by replacing (A.6) and (A.7) into (A.4), (10) can be achieved.

REFERENCES

[1] H. Günther, "NMR spectroscopy: basic principles, concepts and applications in chemistry", John Wiley & Sons, 2013.

[2] J.C. Visschers, E. Wilson, T. Connelly, A. Mudrov, L. Bougasi, "Rapid parameter determination of discrete damped sinusoidal oscillations", Optics Express, vol. 29, no. 5, 2021, pp. 6863-6878.

[3] K. Duda, T. P. Zielinski, L. B. Magalas, M. Majewski, "DFT based estimation of damped oscillation's parameters in low frequency mechanical spectroscopy", IEEE Trans. Instrum. Meas., vol. 60, no. 11, Nov. 2011, pp. 3608–3618.

[4] E. Aboutanios, "Estimation of the frequency and decay factor of a decaying exponential in noise", IEEE Trans. Signal Process., vol. 58, no. 2, Feb. 2010, pp. 501–509.

[5] M. Bertocco, C. Offeli, D. Petri, "Analysis of damped sinusoidal signals via a frequency-domain interpolation algorithm", IEEE Trans. Instrum. Meas. vol. 43, no. 2, Apr. 1994, pp. 245–250.

[6] K. Wang, H. Wen, L. Xu, L.Wang, "Two Points Interpolated DFT Algorithm for Accurate Estimation of Damping Factor and Frequency", IEEE Signal Process. Letter, vol. 28, 2021, pp. 499-502.

[7] R. Diao, Q. Meng, "An interpolation algorithm for discrete Fourier transforms of weighted damped sinusoidal signals", IEEE Trans. Instrum. Meas., vol. 63, no. 6, June 2014, pp. 1505–1523.

[8] R. Diao, Q. Meng, H. Fan, "Interpolation algorithms based on Rife-Vincent window for discrete Fourier transforms of damped signals (in Chinese)", Journal of Mechanical Engineering, vol. 51, no. 4, Feb. 2015.

[9] D. Belega, D. Petri, "Fast interpolated DTFT estimators of frequency and damping factor of real-valued damped sinusoids", Measurement, vol. 217, Aug. 2023.

[10] F.J. Harris, "On the use of windows for harmonic analysis with the discrete Fourier transform", Proceedings of the IEEE, vol. 66, no. 1, Jan. 1978, pp. 51–83.

[11] A.H. Nuttall, "Some windows with very good sidelobe behavior", IEEE Trans. Acoust. Speech Signal Process., vol. ASSP-29, no. 1, Feb. 1981, pp. 84–91.

[12] E. Jacobsen, P. Kootsookos," Fast, accurate frequency estimators", IEEE Signal Process. Mag., vol. 24, May 2007, pp. 123-125.

[13] C. Candan, "A method for fine resolution frequency estimation from three DFT samples", IEEE Signal Process. Lett., vol. 18, no. 6, June 2011, pp. 351-354.

[14] D. Belega, D. Petri," Frequency estimation by two- or three-point interpolated Fourier algorithms based on cosine windows", Signal Process., vol. 114, 2015, pp. 115-125.

[15] Y. Yao, S.M. Pandit, "Cramér-Rao lower bounds for a damped sinusoidal process", IEEE Trans. Signal Process., vol. 43, no. 4, Apr. 1995, pp. 878–885.

[16] E. Aboutanios, "Estimating the parameters of sinusoids and decaying sinusoids in noise", IEEE Instrum. Meas. Mag., vol. 14, no. 2, Apr. 2011, pp. 8–14.